

Electrochemical Degradation Pathways of 1,1,1-Trichloroethane by Immobilized P450 CYP119 in Extreme Temperature and pH Environments

by Emek Blair

Extremophilic organisms live under conditions which are, from a human perspective, deadly. For instance, the archaeobacteria *Sulfolobus solfataricus*, lives happily at *ca.* 80°C in sulfurous volcanic springs of *~* pH 3.5. Because of stability under extreme conditions, enzymes from such organisms are of interest as catalysts in industrial applications. Toward such a goal, our group has previously reported the use of a cytochrome P450, CYP119, from the genome of *S. solfataricus*, as an electrocatalyst on surface-modified electrodes. This thermophilic heme protein has a denaturation point of *~*90°C and is resistant to extremes of pH and pressure for extended periods.¹ CYP119 gives an excellent electrochemical response when immobilized in a surfactant film on pyrolytic graphite electrode (PG),² a methodology first developed by the Rusling group.³ CYP119 proved to be a superior catalyst for multi-electron reductions of NO_x species such as nitrite and nitric oxide,⁴ as well for dehalogenations of C₁ chlorocarbon solvents.⁵

Chloro-organics are mutagenic and hepatotoxic, being metabolized into carcinogens by P450 enzymes in the human liver.⁶ As these compounds are produced on the billion of pounds per year scale, high concentrations are found in virtually all of the EPA's hazardous waste sites.⁷ We have previously used CYP119 to electrocatalytically degrade CCl₄ to CH₄ at temperatures exceeding 75°C, immobilized in dimethyldidodecyl-ammonium poly(*p*-styrenesulfonate) (DDAPSS).⁵ Due to the extended stability of this modification method, previously inaccessible conditions of pH and temperature may now be electrochemically investigated. In this work we explore the complex catalytic dechlorination of 1,1,1-trichloroethane (MeCCl₃) by CYP119/DDAPSS, specifically examining changes in turnover and product distribution upon variations in temperature, pH, and electrolysis potential.

Our initial report described the dramatic effect of temperature on the Fe^{III/II} couple of CYP 119, which shifts negatively > 1 mV/°C;⁵ variation of pH was found to shift the Fe^{III/II} and Fe^{II/I} couple by *ca.* -50 and -10 mV per pH unit. Catalytic reduction of MeCCl₃ is seen at the Fe^{III/II} couple but is greatly enhanced at the Fe^{II/I} couple. As expected, increasing the temperature increases the catalytic current, with turnover rates of *ca.* 4,

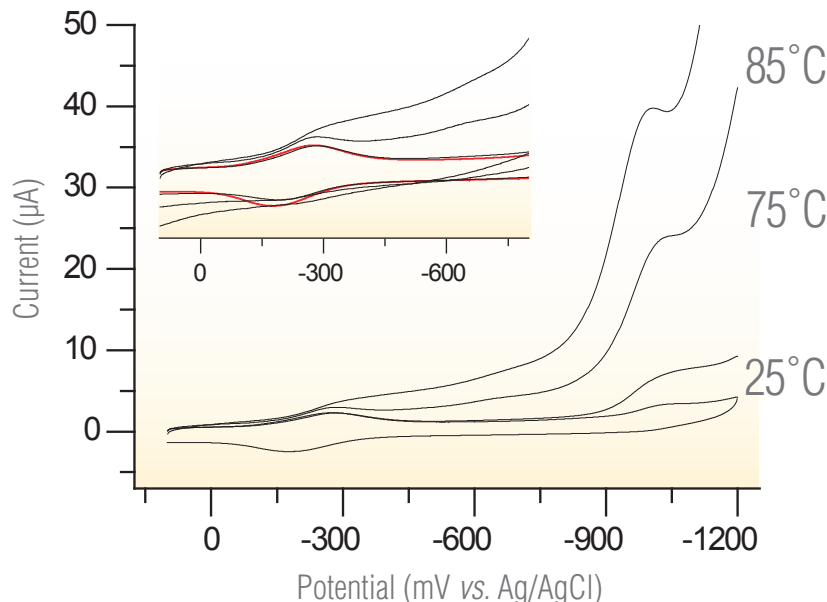


Fig. 1. Temperature effects on 1,1,1-trichloroethane electrocatalytic dehalogenation. Linear sweep voltammograms of DDAPSS/CYP119 in the presence of saturated MeCCl₃ at 25, 55, and 85°C. A cyclic voltammogram of DDAPSS/CYP119 in 50 mM pH 7 iP buffer scanned at 200 mV/s using a PG working electrode, Pt mesh counter electrode, and isothermal Ag/AgCl 3M KCl reference electrode is included as a reference. (Inset) Magnified view of Fe^{III/II} catalytic wave (red is without MeCl₃).

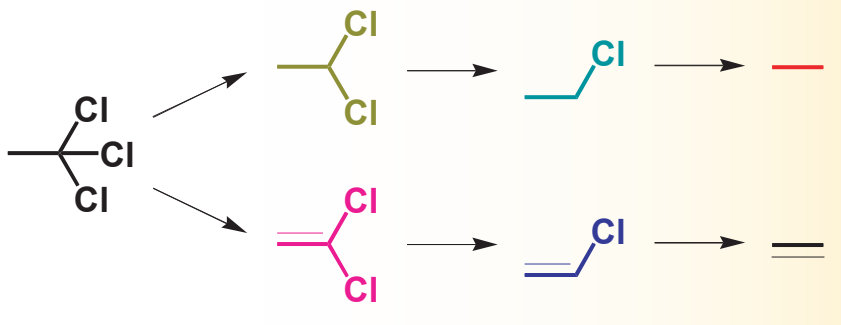


Fig. 2. Electrolysis products of 1,1,1-trichloroethane (figure not indicative of mechanistic pathway). The color scheme matches Fig. 3.

14, and 22 s⁻¹ observed at 25, 55, and 85°C, respectively (Fig. 1); the halfwave potential of the highest catalytic wave shifts from *ca.* -960 mV at 25°C pH 7 to *ca.* -920 mV at 85°C. The catalytic current at Fe^{III/II} couple also increases with temperature, and a corresponding loss of reversibility (inset Fig. 1). Likewise, the catalytic current increases and shifts to more positive potential at lower pH (-1015 mV at pH 10 at 25°C).

One goal of this work is to define conditions that maximize yields of non-chlorinated products. Products generated in CYP119/DDAPSS catalyzed bulk electrolysis of MeCCl₃ were analyzed by gas chromatography - mass

spectrometry or gas chromatography - flame ionization detection (Fig. 2); no products of radical coupling (*e.g.*, C₄) were observed. For both pH 7 and pH 10, reduction at -700 mV yielded the highest percent of the non-chlorinated products (Fig. 3), though at dramatically lower turnover rates. Furthermore, catalysis in pH 10 buffer solutions gave better dechlorination efficiencies, and the greatest overall production of ethane occurred at the 55°C pH 10 buffered solutions. In all cases, the major product is either 1,1-dichloroethane or ethane, again demonstrating the utility of this extremophilic enzyme in multi-electron reductions. Ongoing work addresses mechanistic questions regarding these

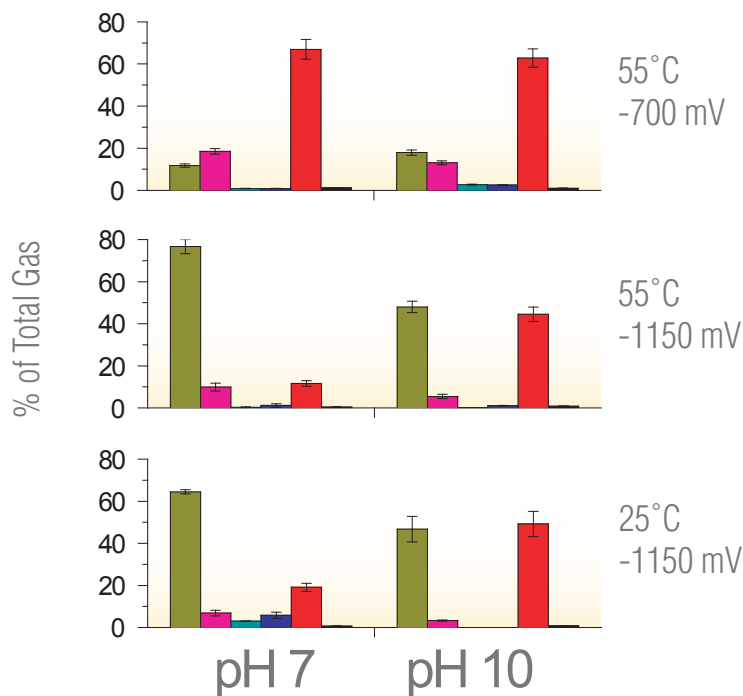


FIG. 3. Potential, pH, and temperature effects on product evolution: (green) 1,1-dichloroethane, (pink) 1,1-dichloroethylene, (turquoise) chloroethane, (blue) vinyl chloride, (red) ethane, and (black) ethylene. Conditions: 50 mM pH 7 iP buffer or 50 mM pH 10 potassium carbonate/potassium tetraborate buffer held at a single potential for 20 min, using a PG working electrode, Pt mesh counter electrode, and an isothermal Ag/AgCl 3M KCl reference electrode.

dechlorination reactions and will be presented in a subsequent publication. ■

Acknowledgments

The author thanks The Electrochemical Society for the Edward G. Weston Summer Research Fellowship and Patrick J. Farmer for his guidance and encouragement.

References

- (a) J. K. Yano, L. S. Koo, D. J. Schuller, H. Li, P. R. Ortiz de Montellano, and T. L. Poulos, *J. Biol. Chem.*, **275**, 31086 (2000); (b) L. S. Koo, R. A. Tschirret-Guth, W. E. Straub, P. Moenne-Loccoz, and T. M. Loehr, *J. Biol. Chem.*, **275**, 14112-14123 (2000); (c) M. A. McLean, S. A. Maves, K. E. Weiss, S. Krepich, and S. G. Sligar, *Biochem. Biophys. Res. Commun.*, **252**, 166 (1998).
- L. S. Koo, C. E. Immoos, M. S. Cohen, P. J. Farmer, and P. R. Ortiz de Montellano, *J. Am. Chem. Soc.*, **124**, 5684 (2002).
- J. F. Rusling, *Acc. Chem. Res.*, **31**, 363 (1998).
- C. E. Immoos, J. Chou, M. Bayachou, E. Blair, and P. J. Farmer, *J. Am. Chem. Soc.*, **126**, 4934 (2004).
- E. Blair, J. Greaves, and P. J. Farmer, *J. Am. Chem. Soc.*, **126**, 8632 (2004).
- U.S. Department of Health, Education, and Welfare, *Environ. Health Perspective*, **21**, 1 (1977).
- P. J. Chenier, *Survey of Industrial Chemistry*, 2nd Revised ed., p. xii, Wiley-VCH, New York (1990).

About the Author

EMEK BLAIR is a fifth year PhD candidate at the University of California, Irvine under the direction of Patrick J. Farmer. He may be reached at eblair@uci.edu.

THE 2005 F. M. BECKET SUMMER RESEARCH FELLOWSHIP SUMMARY REPORT

The Role of Silicon Interstitials in Arsenic-Doped Ultrashallow Junction Formation

by Scott A. Harrison

By the year 2008, it is predicted by the *International Technology Roadmap for Semiconductors* that shallow doped regions less than 10 nm in depth will be necessary to produce the next generation of silicon transistors.¹ In addition to the depth requirement, an extremely high percentage of dopants in these ultrashallow junctions must be electrically active in order to maintain low sheet resistance. To meet these requirements, a better understanding of the dopant diffusion and dopant clustering behaviors that underlie these detrimental problems is necessary. In my work, I used density functional theory (DFT) to build a comprehensive understanding of the role of silicon interstitials in determining the behavior of the arsenic dopant during junction processing.

To create a junction, dopants are implanted into the silicon substrate,

which is subsequently annealed to heal the damaged silicon and activate dopants. During annealing, the interaction of arsenic dopants with silicon defects leads to deleterious arsenic behaviors. Until recently, it was widely accepted that the interaction of arsenic dopants with vacancy defects in crystalline silicon was responsible for both observed arsenic transient enhanced diffusion (TED) as well as arsenic clustering which leads to electrical deactivation.²⁻⁴ While arsenic-vacancy complexes are still believed to be responsible for electrical deactivation, more recent experimental results have shown that silicon interstitials may also mediate arsenic TED.⁵

In the first step of my research, I showed that in the presence of an excess of silicon interstitials, arsenic-vacancy complexes would be annihilated

and easily converted to defect-free complexes.⁶ Prompted by our initial results, we attempted to find a diffusing arsenic-silicon interstitial complex. We identified a highly mobile arsenic-silicon interstitial (As-Si_i) pair with a migration barrier of approximately 0.15-0.30 eV that can exist in both the neutral and plus charge state.⁷ Depending on the Fermi level, the binding energy of the As-Si_i pair is 0.3-0.6 eV with respect to a (neutral) Si interstitial and a (positively charged) As atom. Two diffusion pathways along with their corresponding energetics are shown for the neutral As-Si_i pair in Fig. 1.

In addition to investigating the mobility As-Si_i pair, we also examined the possible formation of larger arsenic-silicon interstitial complexes. We found that diffusing silicon interstitials and As-Si_i pairs can bind significantly

(continued on next page)

to the defect-free complexes formed from arsenic-vacancy annihilation to build larger arsenic-silicon interstitial complexes.⁸ In Fig. 2, we show a thermodynamic map of the potential arsenic-defect complexes that may form in the presence of a silicon interstitial supersaturation. Binding events are indicated with arrows along with their corresponding binding energies. During annealing of an ion-implanted wafer, silicon interstitials tend to escape to the surface over time, resulting in a decrease in the interstitial concentration. This in turn leads to the dissolution of larger arsenic-interstitial complexes and will eventually allow for complexes such as As_3 , As_4 , and As_5 to emit lattice silicon atoms and form arsenic-vacancy complexes.

The results presented here provide insight as to how silicon interstitials may influence arsenic behavior during ion-implanted junction formation and will allow for more detailed kinetic models of junction processing. In addition, these insights should allow for the development of defect engineering and co-doping approaches to reduce arsenic TED, as well as arsenic agglomeration. ■

Acknowledgments

The author thanks The Electrochemical Society for the F. M. Becket Summer Fellowship as well as Gyeong S. Hwang and Thomas F. Edgar for their guidance. In addition, the National Science Foundation is acknowledged for their support in the form of a graduate fellowship as well as the Texas Advanced Computing Consortium for use of their computing resources.

References

1. *International Technology Roadmap for Semiconductors, 2003 ed.*, WWW Document (<http://public.itrs.net/Reports.htm>).
2. A. N. Larsen, K. K. Larsen, P. E. Andersen, and B. G. Svensson, *J. Appl. Phys.*, **73**, 691 (1993).
3. D. W. Lawther, U. Myler, P. J. Simpson, P. M. Rousseau, P. B. Griffin, and J. D. Plummer, *Appl. Phys. Lett.*, **67**, 3575 (1995).
4. M. Ramamoorthy and S. T. Pantelides, *Phys. Rev. Lett.*, **76**, 4753 (1996).
5. A. Ural, P. B. Griffin, and J. D. Plummer, *J. Appl. Phys.*, **85**, 6440 (1999).
6. S. A. Harrison, T. F. Edgar, and G. S. Hwang, *Appl. Phys. Lett.*, **85**, 4935 (2004).
7. S. A. Harrison, T. F. Edgar, and G. S. Hwang, *Appl. Phys. Lett.*, To be published.
8. S. A. Harrison, T. F. Edgar, and G. S. Hwang, *Appl. Phys. Lett.*, Submitted.

About the Author

SCOTT A. HARRISON is a PhD candidate in the Department of Chemical Engineering at the University of Texas at Austin under the direction of Gyeong S. Hwang and Thomas F. Edgar. He may be reached at scotth@che.utexas.edu.

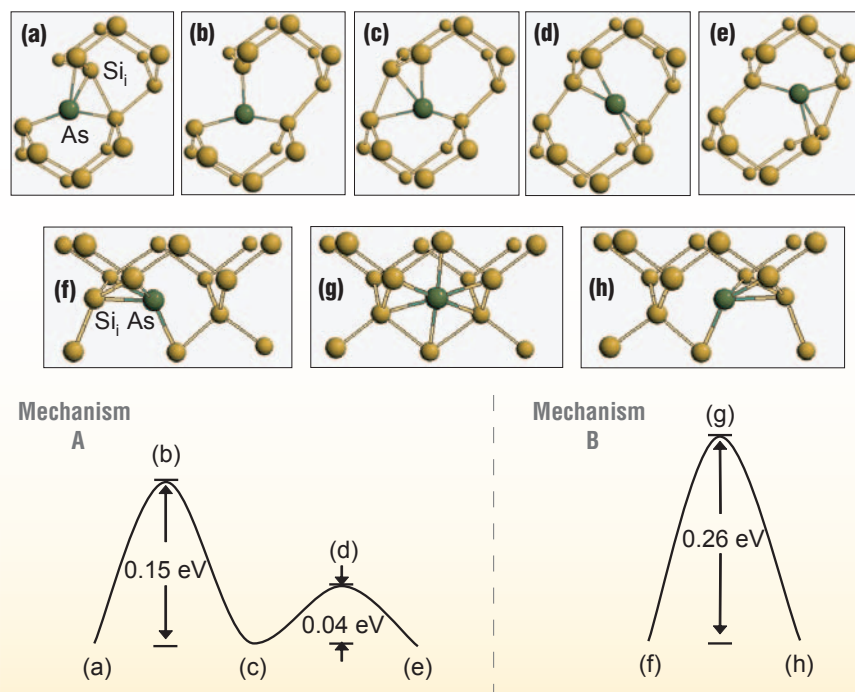


FIG. 1. As-Si_i pair diffusion pathway for mechanism A [(a)-(e)] and mechanism B [structures (f)-(g)] along with the corresponding pathway energetics for the neutral As-Si_i pair. Structures (a), (c), (e), (f), and (h) are minimum energy structures that are equal in energy.

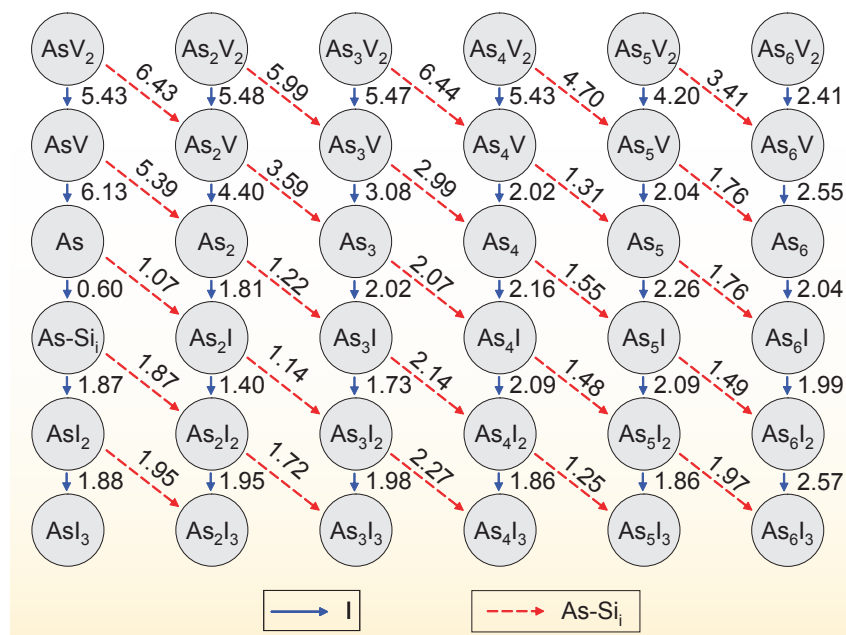


FIG. 2. A thermodynamic map of the potential arsenic-defect complexes that may form in the presence of an interstitial supersaturation. The solid arrows represent the binding of silicon interstitials (I) while the dashed arrows represent the binding of a As-Si_i pairs. The energy for each binding event (in eV) is noted above each arrow.

Effects of the Ligand Chain Length: A Potential Dependence of Charge Transfer over Alkanethiol-Protected Au Nanoparticle Thin Layers

by Georgeta Lica

The solution electrochemistry of alkanethiol-protected Au nanoparticles (NPs) is very well characterized and consists of specific redox-like quantized double layer charging/discharging behavior.¹ However, when thiol-protected Au NP thin layer assemblies are formed on supporting electrodes, interesting new phenomena appear. In a recent report² we have shown that, for a given ligand length (octanethiol), the Au NPs deposited on working electrodes showed different electron transfer properties through the thin layers, which is a function of the particle size (1.7, 2, or 3.5 nm) and the applied potential.

The work over this summer concentrated on the effect of the chain length of the protective monolayer, because this represents another effective control parameter for electron transfer. Hexanethiol, octanethiol, and dodecanethiol-protected Au NPs with similar particle size (about 2 nm) were synthesized using Brust *et al.* method.³ Next, a toluene solution of each sample was drop-cast on a glassy carbon (GC) working electrode. The differential pulse voltammograms (DPVs) of the resulting NP thin layers (Fig. 1) show three different potential ranges: above 0 V where the Coulomb blockade waves can be clearly discerned; between 0 and -0.4 V, where the current drops to the level of the background; and below -0.4 V, where the current starts increasing again. These observations suggest that the thin-film assemblies act like a dielectric material at positive potential, but like a metal in the valley.

This hypothesis has been tested using three compounds whose reversible electrochemical redox properties are well known in these potential ranges: potassium ferricyanide (above 0 V), a polyoxometalate, $\text{SiW}_{12}\text{O}_{40}^{4-}$ (between -0.5 and 0.05 V), and methyl viologen (below -0.5 V). The idea behind these experiments was that any impediment of the electron transfer through the thin-layer assemblies should show up on the reversibility of these systems.

For the ferricyanide system, an increase in the peaks separation as well as the broadening of the cyclic voltammetric (CV) curves were observed with the increase of the chain lengths (Fig. 2a). The corresponding electron transfer kinetic constants determined using Nicholson method⁴ were 3.6×10^{-6} , 2.2×10^{-6} and 5.4×10^{-7} cm/s for the hexanethiol, octanethiol, and dodecanethiol-protected Au NP thin

(continued on next page)

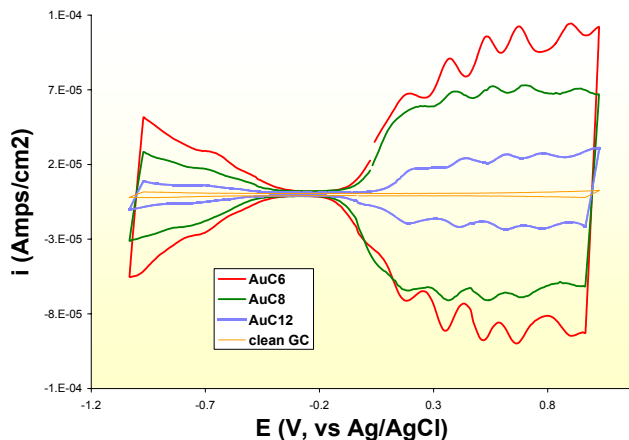


Fig. 1. DPVs of the clean GC working electrode (WE) and of the Au NP thin layers on the GC electrode in 0.5 M $\text{Bu}_4\text{NClO}_4/\text{ACN}$.

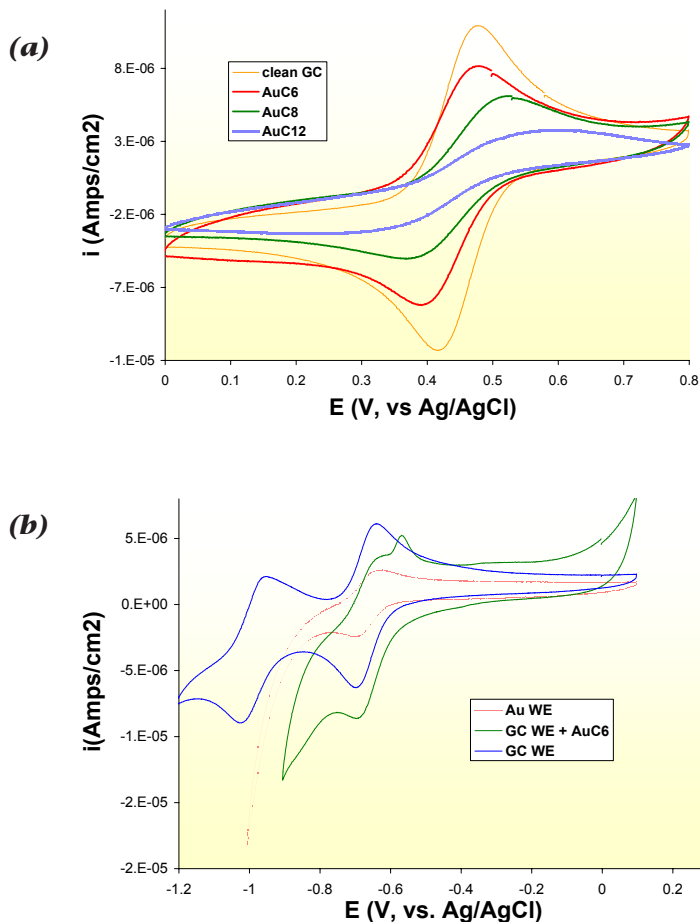


Fig. 2. (a) CVs of the clean GC WE and of the Au NP thin layers on the GC electrode in 1 mM $\text{K}_3\text{Fe}(\text{CN})_6/0.5 \text{ M H}_2\text{SO}_4$ and (b) CVs of a clean GC WE, AuC6 thin layer deposited on GC WE and of a clean Au electrode in 0.1 mM viologen/phosphate buffer pH 7.

layers, showing that a longer chain length causes a stronger impediment in the electron transfer. At the same time, no impediments have been observed for the redox waves of $\text{SiW}_{12}\text{O}_{40}^{4-}$ at -0.24 and -0.5 V. This suggests that the thin-film assemblies appear to be transparent for the electron transfer. Interestingly, in the -0.5 to 1 V range, the thin layer assembly for all three samples behaves similarly to a bare Au electrode, rather than the GC electrode, indicating that the supporting electrode was completely covered (Fig. 2b).

Future work will concentrate on applying these interesting charge transfer properties in gate-transistor devices, for the development of real-world field effect electronics. Shortly, the I-V behavior of the thin-layer assembly of Au NPs connecting the two

electrodes of a transistor-type device will be studied along with function of the gate biased potential, core size, and chain length. ■

Acknowledgments

The author acknowledges The Electrochemical Society for the Colin G. Fink Summer Fellowship and YuYe Tong for his guidance through the project. Financial supports from the Georgetown startup fund, PRF fund, and the summer grant, pilot research grant, and grant-in-aid from Georgetown Graduate School are gratefully acknowledged.

References

1. S. Chen and R. W. Murray, *J. Phys. Chem.*, **97**, 332 (1993).
2. G. C. Lica and Y. Y. Tong, Paper 222 presented at The Electrochemical Society Meeting, Honolulu, HI, Oct. 3-8, 2004.

3. M. Brust and C. J. Kiely, *Colloids and Surfaces*, **202**, 175 (2002).
4. R. S. Nicholson, *Anal. Chem.*, **37**, 1351 (1965).

About the Author

GEORGETA LICA is a PhD candidate in the Department of Chemistry, Georgetown University under the direction of YuYe Tong. She may be reached at gcl4@georgetown.edu.

THE 2004 JOSEPH W. RICHARDS SUMMER FELLOWSHIP SUMMARY REPORT

Fabrication of Colloidal Nanostructures from Nanolithographically Defined Templates

by Khalid Salaita

Over the past century, colloidal chemists have painstakingly developed methods to synthesize monodisperse metal particles of various sizes and compositions and these have subsequently been found useful for applications in fields ranging from bio-detection to catalysis.^{1,2} Interestingly the properties of nanoparticles are not only dependent on size and composition but they are also heavily dependent on shape.³ However, synthetic chemists encounter great difficulty in realizing novel methods of generating monodisperse particles that are also anisotropic. For example, star shaped particles may never be synthesized by solution-based methods. On the other hand, electrochemical deposition methods offer a number of advantages to generating metal nanostructures on surfaces, because these techniques are simple, routinely applicable, and can be finely controlled down to the single atomic layers.⁴ As an example Penner *et al.* have studied the preferential nucleation and growth of nanoparticles and nanowires at graphite defects and step edges.⁵ In this work, we hypothesized that intentionally nano-patterned surfaces could control the selective nucleation and growth of metallic nanostructures of virtually any shape or geometry. Dip-pen nanolithography (DPN), a scanning probe-based lithographic technique developed by our group, that is readily amenable for parallelization,⁶ can be used to chemically functionalize surfaces down to the 15-nm scale.^{7,8}

In previous work, we demonstrated that alkanethiol and alkaneselenide

nanostructures deposited onto a Au surface can be electrochemically desorbed or whittled from the periphery inward under the influence of a negative potential.^{9,10} By simply changing the head or tail group of an adsorbate, their desorption potential could be

tuned. For example, we found that 16-mercaptohexadecanoic acid (MHA) molecules can be electrochemically whittled when a Au patterned substrate is placed into a 0.5 M KOH solution and a -750 mV potential is applied vs. an Ag/AgCl electrode. However, we also

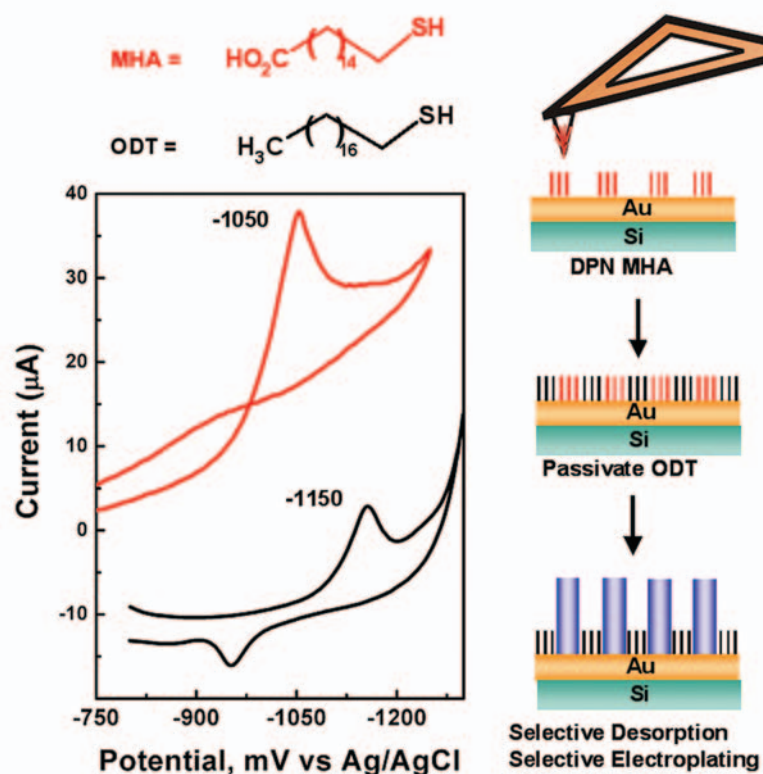


Fig. 1. Cyclic voltammogram of the reductive desorption of MHA and ODT monolayers formed on polycrystalline Au films in 1 M KOH. Ag/AgCl and Pt wires were used as reference and counter electrodes, respectively. Schematic illustration shows the process of selective desorption and metal deposition on DPN-generated nanoscale templates.

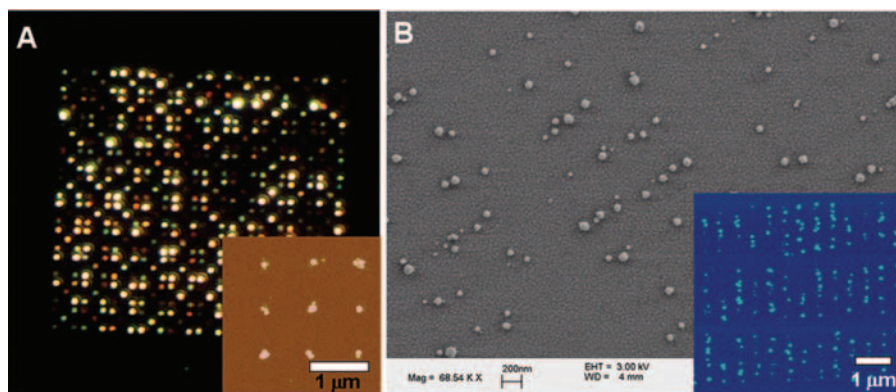


Fig. 2. (A) Dark field optical micrograph of an array of Ag particles deposited onto 100 nm MHA dot templates, inset shows non-contact AFM image of 9 MHA dots after Ag deposition. (B) SEM image of Pt particles electrodeposited on MHA line templates, inset shows non-contact AFM image of same array of particles.

found that the onset of desorption for 1-octadecanethiol (ODT) is significantly more negative, and a potential of -950 mV vs. an Ag/AgCl reference electrode is required to initiate desorption (Fig. 1). We hypothesized that this difference in onset of reductive desorption would be enough to selectively displace the acid terminated MHA molecules, and reductively deposit metal salts in its place (Fig. 1).

To test this scheme, 100 nm MHA dot templates were generated onto a Au substrate. By following the procedures described in Fig. 1 and applying a potential of -790 mV vs. Ag/AgCl, nucleation and growth of Ag nanoparticles from a Ag plating solution selectively occurred onto the MHA template, Fig. 2A. Both dark-field

microscopy and atomic force microscopy imaging, Fig. 2A, indicate that there are a number of different shapes and sizes of particles formed. MHA line templates also provide nucleation sites for the growth of Pt nanoparticles when a potential of -650 mV vs. Ag/AgCl is applied, Fig. 2B. Although high selectivity was achieved using this method, particle nucleation occurred nonuniformly across the MHA patterned areas.

In conclusion, a method has been developed to control the selective nucleation and growth of metal nanoparticles onto lithographically defined templates. With the help of ECS, we have realized a novel strategy to generate metal nanoparticles on patterned substrates. Future work will

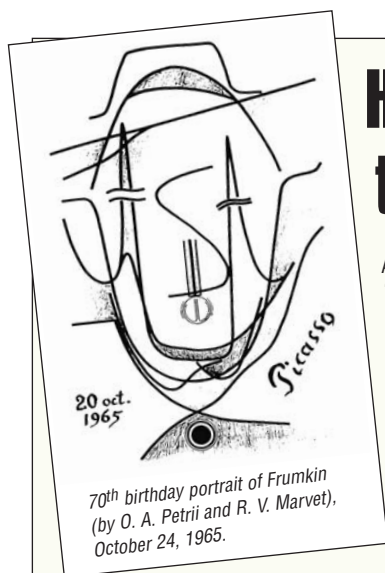
involve using surface characterization tools such as X-ray photoelectron spectroscopy, and Fourier transform infrared spectroscopy to probe the process of selective desorption of alkanethiols from Au substrates. ■

References

1. N. L. Rosi, C. A. Mirkin, *Chem. Rev.*, **105**, 1547 (2005).
2. M. C. Daniel and D. Astruc, *Chem. Rev.*, **104**, 293 (2004).
3. C. J. Murphy, T. K. San, A. M. Gole, C. J. Orendorff, J. X. Gao, L. Gou, S. E. Hunyadi, and T. Li, *J. Phys. Chem. B*, **109**, 13857 (2005).
4. L. D. Qin, S. Park, L. Huang, and C. A. Mirkin, *Science*, **309**, 113 (2005).
5. F. Favier, E. C. Walter, M. P. Zach, T. Benter, and R. M. Penner, *Science*, **293**, 2227 (2001).
6. K. Salaita, S. W. Lee, X. Wang, L. Huang, T. M. Dellinger, C. Liu, and C. A. Mirkin, *Small*, **1**, 940 (2005).
7. D. S. Ginger, H. Zhang, and C. A. Mirkin, *Angew. Chem. Int. Ed.*, **43**, 30 (2004).
8. R. D. Piner, J. Zhu, F. Xu, S. H. Hong, and C. A. Mirkin, *Science*, **283**, 661 (1999).
9. Y. Zhang, K. Salaita, J. H. Lim, and C. A. Mirkin, *Nano Letters*, **2**, 1389 (2002).
10. Y. Zhang, K. Salaita, J. H. Lim, K. B. Lee, and C. A. Mirkin, *Langmuir*, **20**, 962 (2004).

About the Author

KHALID SALAITA is a PhD candidate in the Department of Chemistry and Institute for Nanotechnology, Northwestern University, under the guidance of Chad A. Mirkin. He may be reached by e-mail at ksalaita@chem.northwestern.edu.



Historical Perspectives on the Evolution of Electrochemical Tools

At the 201st ECS meeting in Philadelphia in May 2002, the Physical Electrochemistry Division organized a symposium, entitled "Progress in Methods Used to Solve Electrochemical Problems: Historical Perspectives." Using an unorthodox approach in preparing a publication based on this symposium, the organizers taped the lectures of the five invited senior leaders in the field (B. E. CONWAY, A. T. HUBBARD, W. R. HEINEMAN, D. M. KOLB AND R. W. MURRAY), who were the keynote speakers, and later transcribed their talks into articles suitable for a symposium volume. This volume is now available.

In addition to the five long chapters, the volume also includes sixteen vignettes from other key researchers and members of the Physical Electrochemistry Division. (F. C. ANSON, A. J. BARD, J. O'M. BOCKRIS, W. R. FAWCETT, S. W. FELDBERG, A. HELLER, P. T. KISSINGER, Z. NAGY, K. NIKI, M. G. HILL, H. B. GRAY, K. B. OLDHAM, G. N. PAPANATHANAKIS, P. N. ROSS JR., W. VIELSTICH, M. J. WEAVER, AND P. ZUMAN.) J. LEDDY, the lead editor, prepared an introductory chapter to the volume, providing the scientific lineage of the many contributors and including other items of great interest.

This symposium volume will be of historical and scientific interest to all members of ECS, serving both as a fascinating summary of personal experiences and historical breakthrough research in physical electrochemistry, as well as a powerful teaching aid for undergraduate and graduate courses in electrochemistry.

SV 2002-29—Historical Perspectives on the Evolution of Electrochemical Tools, Editors: J. Leddy, V. Birss, and P. Vanysek, ISBN 1-56677-383-0, 348 pages, ECS member price \$78.00, nonmember price \$94.00

The Electrochemical Society

65 South Main Street, Building D, Pennington, NJ 08534-2839, USA
Tel: 609.737.1902 • Fax: 609.737.2743 • E-mail: orders@electrochem.org